BREAKAGE MATRIX COMPARISON OF GRANULATED FOOD PRODUCTS FOR PREDICTION OF ATTRITION DURING LEAN-PHASE PNEUMATIC CONVEYING

B.A. Kotzur[(a)], M.S.A. Bradley[(b)], R.J. Berry[(c)], R.J. Farnish[(d)]

[(a),(b),(c),(d)]The Wolfson Centre for Bulk Solids Handling Technology, University of Greenwich, United Kingdom

[(a)]B.A.Kotzur@greenwich.ac.uk, [(b)] M.S.A.Bradley@greenwich.ac.uk, [(c)] R.J.Berry@greenwich.ac.uk, [(d)]R.J.Farnish@greenwich.ac.uk

EXTENDED ABSTRACT

1. INTRODUCTION

Pneumatic conveying is widely used in the production and handling processes of many food products. These food products can take the form of powders or flake type bulk materials, including items such as tea leaves, granulated sugar, flour, and flavorings. The main advantages of using pneumatic conveying to transport materials throughout a process include the maintenance of product hygiene, and the potential for flexibility in pipework routing in comparison to mechanical conveying. However, the fulfilment of the many benefits of pneumatic conveying can only be realised if the system is correctly configured and operated optimally. In instances where this is not the case, a common repercussion, is bulk material attrition due to excessive impact forces exerted on the particles as they pass through the system, and encounter changes in direction at bends. The final result can often be the generation of excess quantities of degraded particle size fractions – often in the form of fines or dust. The presence of these smaller particle sizes can have significant implications for the reliability of subsequent process operations or customer perception.

1.1. Motivation

The research presented in this document will provide a comparative breakage analysis of two types of food products, one crystalline in structure, and the other non-crystalline. This information may then be used to predict with a greater degree of confidence, the magnitude of anticipated attrition when pneumatically conveying particulate materials.

1.2. Lean Phase Pneumatic Conveying

There are three main modes of pneumatic conveying:

1. Dense-phase.
2. Lean-phase.
3. Pulse/dune flow.

Mode 1 describes conveying conditions when the entire cross-section of the pipe is occupied by particles at relatively low velocity (approximately 2-8 m/s). Mode 2 describes conveying conditions when the particles are fully suspended in the air flow under high velocity conditions (greater than approximately 12 m/s). Mode 3 describes transient conveying conditions between Modes 1 and 2, and describes the flow of ‘dunes’ of material progressing through the pipeline.

This study will consider lean phase pneumatic conveying effects specifically, as the combination of high velocity and low particle concentration yields the most likely conditions to induce an increased level of particle attrition.

1.3. Repercussions of excess fines content

The term ‘fines’ in this research shall refer to the d_{10} content of the virgin cumulative size distribution. Should the material within this size range make up too large a proportion of the overall mass, adverse material handling and performance issues can occur. These types of issues are extensive, and include:

- Unreliable discharge from hoppers,
- Dust generation, leading to explosion or health hazards,
- Segregation of mixtures,
- Excess dust in commercial products leading to customer complaints,
- Error in volumetric dosing operations due to variations in bulk density.

The occurrence of such issues typically results in additional time and financial costs to the producers of the product. These costs are consumed in amending the configuration or operating conditions of the existing process, or in reformulating the nature of the material handled.

1.4. Advantages of predictive analysis

This research seeks to provide an improved tool that can be applied to identify risk within processes. The approach will use predictive analysis of the product through empirical testing. Particle impact conditions can be carefully controlled within a centrifugal accelerator attrition tester, to provide comparative data

for qualitative analysis. Then, based on a comparison with products previously handled, insight into the breakage behavior may be attained and its subsequent attrition behavior estimated.
A selection of advantages that predictive analysis would yield include:

- Reduced requirement for post-installation troubleshooting,
- Enhanced understanding of the operating parameters that cause an unacceptable degree of attrition,
- Heightened stakeholder awareness of the nature of the material, with regard to particle attrition.

2. LITERATURE

There has been significant research conducted into lean phase pneumatic conveying, with respect to the erosion of pipeline bends. A number of models exist which seek to predict the level of erosion through modelling and empirical testing (Burnett 1996; Deng 2005; Macchini 2013; Sato 1995). As an issue that is closely related to erosion, there is presently a lack of research focusing solely on modelling of attrition of bulk material particles during lean phase pneumatic conveying.
Kalman (2000) conducted an extensive programme of pneumatic conveying tests, exploring the effect of a wide number of parameters on the attrition of various bulk materials. The equipment used in this study has the potential to cause particle attrition, and this has been addressed in the manuscript. The output of the research is limited to general relationships and recommendations in limiting the degree of particle attrition caused by a pneumatic conveying system.
Bridle (2000) performed an in-depth study of particle attrition through the testing and comparison of results between two testing facilities: a single bend test apparatus, and an industrial scale apparatus. The drawbacks of this study were that only three bulk materials were considered: granulated sugar, basmati rice, and malted barley. In addition to this, the testing programme did not consider the attrition behavior of narrow size fractions, nor could the test be performed in a conventional laboratory due to floor space requirements.
Chapelle P (2004) demonstrated a method for taking measurements from a bench top tester and scaling them up to predict the particle attrition behavior in an industrial-scale pneumatic conveying system. While this work lays the foundation for obtaining a scale-up procedure from a bench top scale, the range of variables for this form of testing were not fully explored, omitting the effect of solids loading ratio and impact angle. Additionally, a 5 gram sample was used, making the data exceedingly sensitive to variation in sample size distribution.
van Laarhoven, (2012) developed a new attrition tester of a scale suitable for placement on a laboratory desk. This tester contained the test sample within an oscillating box, where the particles would impact against the walls, causing attrition. Impact velocities estimated to be in the order of 1-5 m/s were attained. The significantly larger impact velocities observed in pneumatic conveying systems (up to 40 m/s) were simulated through increasing the number of impacts in the tester. The study was also limited to two granular materials, and tested a wide sample size distribution.

3. METHOD

Section 3 will describe the methods used to acquire the results in this course of research.

3.1. Materials

Two materials were selected for this course of research: golden breadcrumbs, and cooking salt. The former has a non-crystalline structure, and the latter exhibits a crystalline structure. Additionally, each material has a significantly different size distribution, with respect to the mean and range of particle sizes.

3.2. Statistically Representative Sampling

Due to the generally highly variable nature of bulk materials, it is essential that the testing be conducted using statistically representative samples obtained from the master batch. Should this prerequisite be neglected, subsequent tests could be conducted using samples with significant variation in size distribution or mixture composition. Therefore, statistical subdivision was conducted through the use of two apparatuses: a spinning riffler and riffle boxes.

3.2.1. Spinning Riffler

This piece of equipment is used for statistically subdividing samples of up to 40 litres in volume and is depicted in Figure 1.

Figure 1: Spinning Riffler

A mass-flow hopper is positioned above a vibratory feeder, which in turn dispenses the bulk material master sample into eight sub-samples on a rotating carousel. The amplitude of the vibratory feeder can be varied to

control the bulk material dispensary rate. This method produces eight statistically representative samples from a master sample.

3.2.2. Riffle Boxes

Riffle boxes are used for statistical subdivision of sample sizes up to approximately 500 millilitres. Figure 2 depicts the riffle boxes used for this programme of research.

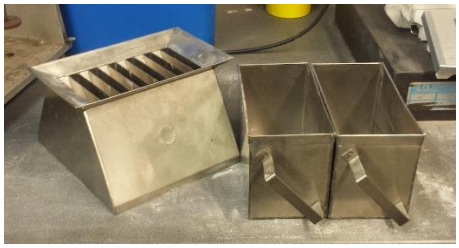

Figure 2: Riffle Boxes

Material is poured into the top of the separating section, which contains a series of slots, alternating between two receiving vessels underneath. This method produces two statistically representative samples from a master sample.

3.3. Particle Size Measurement

In order to determine the virgin size distribution of the sample and the post-test size distribution, a stack of mechanical sieves was used. These were cleaned in an ultrasonic bath prior to use in order to remove any contaminants.

The sieve size progression chosen for this course of research followed a $\sqrt{2}$ progression increase in aperture size. Due to the interest in the smaller size fractions generated, as detailed in the introduction, the sieve progression will begin at the smallest size of 45 µm. This will enable closer inspection of the material residing within small size fractions generated as a result of the degradation testing.

The bulk material sample was loaded into the top of the sieve stack, after which the stack was placed on a vibrating plate, depicted in Figure 3. The subsequent sieving was performed for 15 minutes.

Once sieving was complete, a set of electronic scales was used to determine the mass retained on each sieve to the nearest 0.01 g.

3.4. Attrition Test

The attrition testing was performed on a centrifugal accelerator style attrition tester, depicted in Figure 3.

Figure 3: Centrifugal Attrition Tester

The sample material is inserted into the upper mass-flow hopper of the apparatus. It is then fed into the tester below via an increasing-capacity screw. The rate of screw rotation was kept constant throughout the course of the testing, and consistency in material delivery rate was stable. The function of the screw feeder is to ensure that the volumetric flow rate of material into the attrition test is controlled – a trait that is not closely controlled in many forms of attrition testing.

The material fed from the screw feeder then enters the center of a rotating spindle, and accelerated outwards through a series of radial tubes. The accelerated particles then impact with a target array at a known angle of impact.

The post-test sample is collected at the base of the impact chamber, and taken for size analysis.

3.4.1. Sample Preparation

To obtain the required sample size for each test, the master sample was riffled down to a suitable size for separation via mechanical sieving. In the knowledge that each material batch fed into the sieving unit is statistically representative of the master sample, the size fraction retained on each sieve may also be treated as statistically representative samples. Therefore, samples of known size range with upper and lower bounds may be prepared for testing in the centrifugal accelerator attrition tester.

4. RESULTS

The results for this course of research consist of the initial virgin size distribution, the resultant size distributions when a statistically representative sample is degraded under known conditions, and the resultant size distribution when a known size fraction of material is degraded under known conditions.

It should be noted that the value of '0 µm' for the sieve size represents the material retained in the pan at the base of the sieve stack.

4.1. Virgin Size Distribution

The initial analysis undertaken was to determine the virgin size distribution of the 16 kg master sample for

golden breadcrumbs and salt, presented in Figure 4 and Figure 5 respectively.

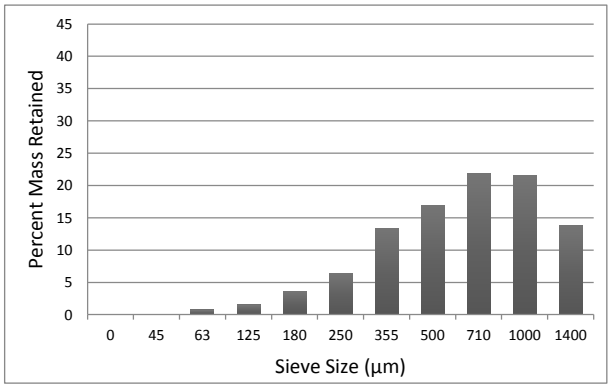

Figure 4: Virgin Size Distribution of Golden Breadcrumbs

No particles used for testing were retained on a 2000 µm sieve – the next sieve in the √2 progression.
Though inspection of the size distribution of golden breadcrumbs, the three size fractions representing the largest proportions of material by mass were chosen to undergo narrow size fraction degradation tests. These size fractions consist of the material retained on 500, 710 and 1000 µm sieves. These fractions represent approximately 58% of the total sample distribution by mass.

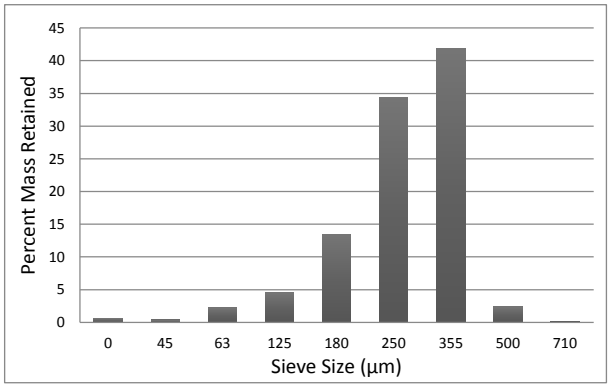

Figure 5: Virgin Size Distribution of Salt

No particles used for testing were retained on a 1000 µm sieve – the next sieve in the √2 progression.
Through inspection of the size distribution of salt, two size fractions, 250 and 355 µm, were chosen for narrow size fraction degradation testing. These fractions represent approximately 75% of the total sample distribution by mass.

4.2. Size Distribution Post-Breakage

This section presents the results of the degradation tests performed with the full virgin size distribution as the input material. Three velocities were tested: 15, 25 and 35 m/s. The results for the golden breadcrumbs are presented in Figure 6, and the results for the salt are presented in Figure 7.

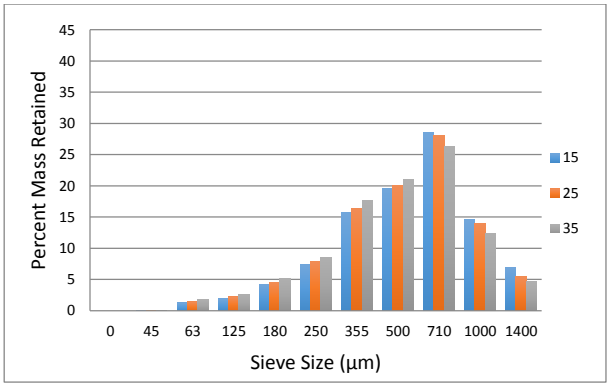

Figure 6: Results of Full Size Distribution Tests under Three Impact Velocities (measured in m/s) for Golden Breadcrumbs

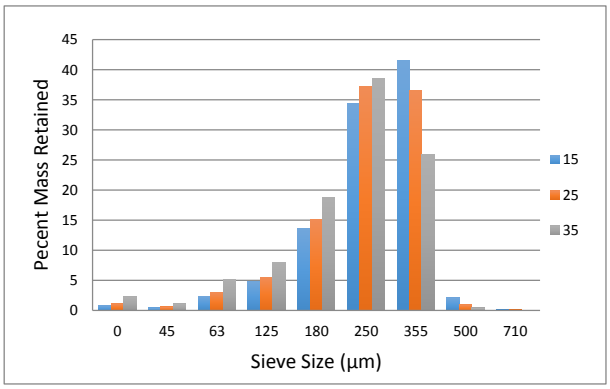

Figure 7: Results of full size distribution tests under Three impact velocities (measured in m/s) for salt

4.3. Narrow-Fraction Size Distribution Post-Breakage

This section presents the results of degradation tests of narrow size fractions across three impact velocities: 15, 25, and 35 m/s. Figures 8, 9 and 10 present the results for golden breadcrumbs, and Figures 11 and 12 present the results for salt, all at impact velocities of 15, 25 and 35 m/s.

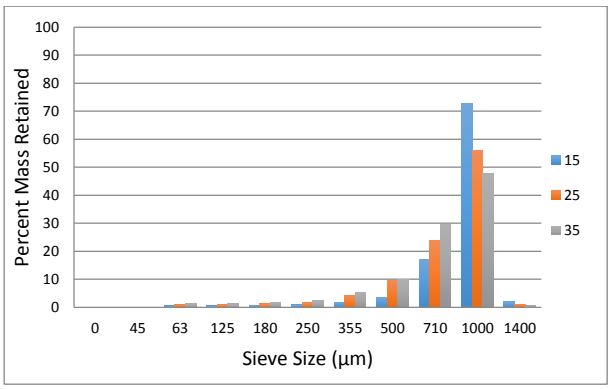

Figure 8: Results of 1000-1400 µm size fraction tests under three impact velocities (measured in m/s) for golden breadcrumbs

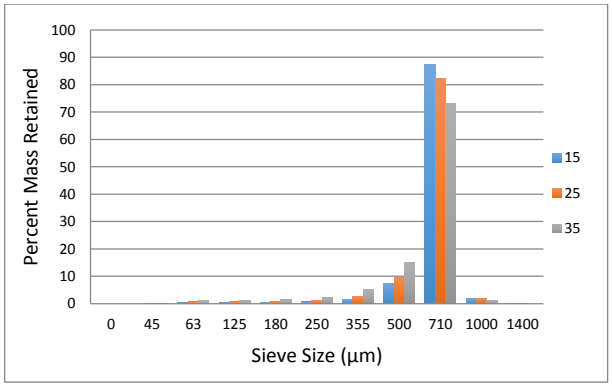

Figure 9: Results of 710-1000 µm Size Fraction Tests under Three Impact Velocities (measured in m/s) for Golden Breadcrumbs

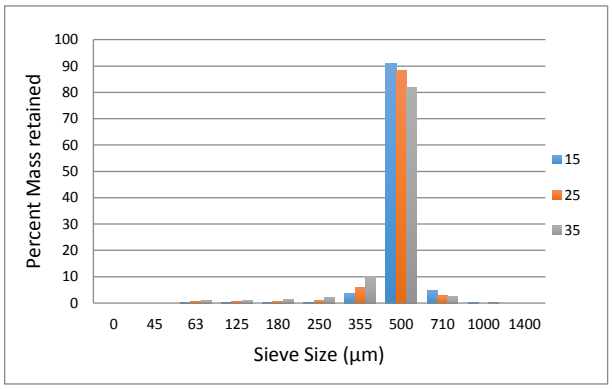

Figure 10: Results of 500-710 µm Size Fraction Tests under Three Impact Velocities (measured in m/s) for Golden Breadcrumbs

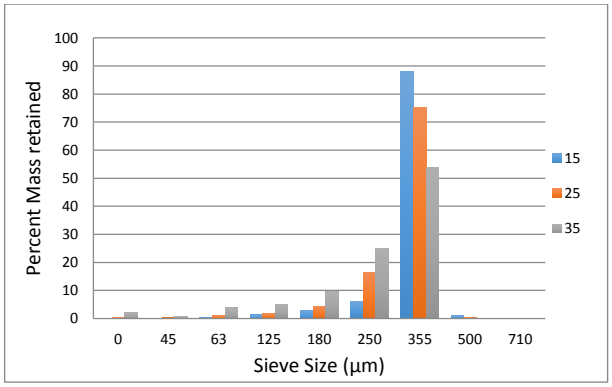

Figure 11: Results of 355-500 µm Size Fraction Tests under Three Impact Velocities (measured in m/s) for Salt

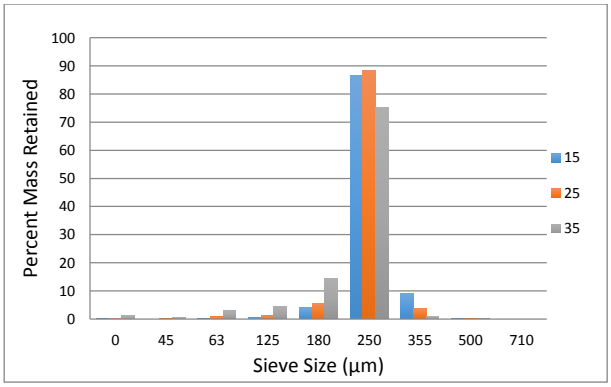

Figure 12: Results of 250-355 µm Size Fraction Tests under Three Impact Velocities (measured in m/s) for Salt

5. DISCUSSION

This section will present the analysis of the results, looking at each of the materials and their representative size fractions in turn.

5.1. Virgin Size Distributions

There are considerable differences observable between the virgin size distributions of the subject materials in this research. Firstly, the golden breadcrumbs exhibit a wider size distribution, where considerable sample mass is clearly spread across seven size fractions from 180 to 1400 µm. Additionally, smaller size fractions are represented with smaller mass percentages. In comparison, the salt exhibited a much narrower overall size distribution, with 75% of the sample by mass residing in two size fractions – on the 250 and 355 µm sieves.

5.2. Full Size Distribution Tests

Observations of the full size distribution tests display behavior typical of attrition tests for most common materials. In the larger size fractions, more mass is retained for low impact velocities in comparison to the high impact velocities. This indicates that more of the larger particles in a sample break under high impact energies. Additionally, it is evident that less mass is retained in the smaller size fractions at low impact velocities in comparison to the higher impact velocities. As expected, an increased number of smaller particles are generated at higher impact velocities.

Figure 13 shows the percentage gain or loss in material for golden breadcrumbs in each size fraction, based on the virgin size distribution for each of the three impact velocities considered.

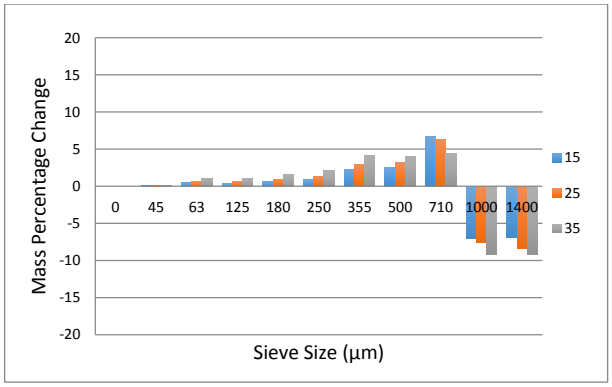

Figure 13: Mass Percentage Change of Golden Breadcrumbs under Impact Velocities (measured in m/s)

The only size fraction that does not follow the expected trend with regards to impact velocity, is the 710 µm sieve. Rather than gaining more material as the impact velocity increases, the reverse is true. This may indicate that this particular size fraction loses more material through particle breakage, than it gains from particle breakage of larger size fractions, namely the 1000 and 1400 µm fractions. By increasing the impact velocity, and hence the impact energy, this behavior is emphasized. Figure 14 presents the results of the same analysis for salt.

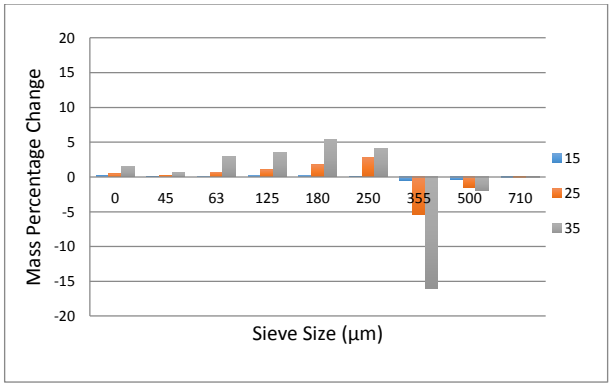

Figure 14: Mass Percentage Change of Salt under Impact Velocities (measured in m/s)

It is evident from the minimal migration of material across the size fractions at 15 m/s, that the impact energy is not sufficient to cause a significant amount of degradation. However, it can be concluded that at 25 and 35 m/s, the impact energy is sufficient to generate smaller particles from the larger size fractions. In particular, large changes are observed at 35 m/s, where a significant proportion of particles undergo size changes.

5.3. Narrow Size Fraction Tests

General observations of the narrow size fraction attrition tests clearly show that larger particles are more susceptible to breakage in comparison to smaller particles for the materials studied. Additionally, the narrow size fractions display similar behavior to that observed in the full size distribution tests, where more particles are broken at higher impact velocities.

Figures 15, 16 and 17 show the percentage change in the size distribution for narrow size fractions of 1000-1400, 710-1000, and 500-710 µm for golden breadcrumbs respectively.

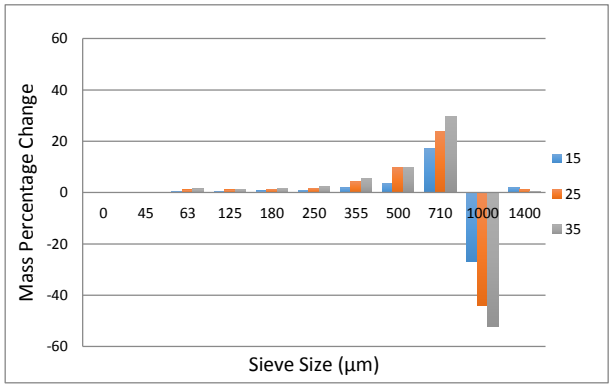

Figure 15: Mass Percentage Change of Golden Breadcrumbs under Impact Velocities (measured in m/s) for the Size Fraction 1000-1400 µm

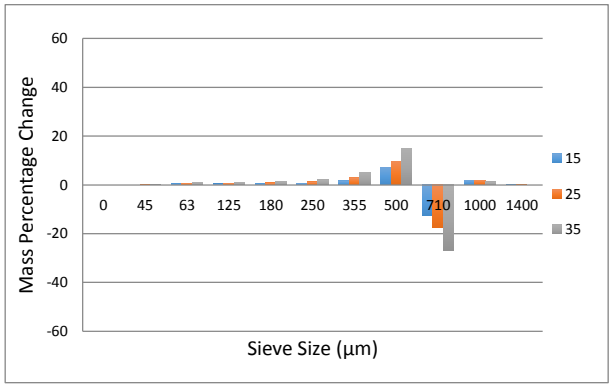

Figure 16: Mass Percentage Change of Golden Breadcrumbs under Impact Velocities (measured in m/s) for the Size Fraction 710-1000 µm

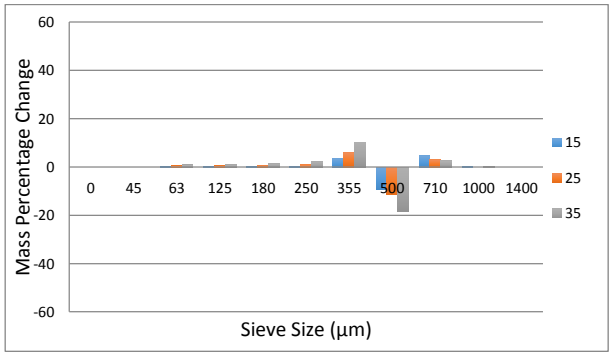

Figure 17: Mass Percentage Change of Golden Breadcrumbs under Impact Velocities (measured in m/s) for the Size Fraction 500-710 µm

This analysis shows some mass retained on sieves larger than the size fraction under scrutiny. This is due to the irregular shape of the particles, which have diameters dependent on the orientation of the particle with respect to the sieve mesh.

In comparing the analysis of three adjacent size fractions for golden breadcrumbs, particle sizes greater than 1000 µm in diameter break to a considerably greater degree than either of those retained on 500 or 710 µm sieves. This suggests that once particles reach 1000 µm in diameter, the particle material does not have enough internal strength to withstand the momentum transfer of the impact. However, with the reduced diameter of the 710 and 500 µm particles, the mass is sufficiently small to maintain the structure of more particles post-impact.
Figures 18 and 19 show the mass percentage change analysis of the 355-500 and 250-355 µm size fractions for salt respectively.

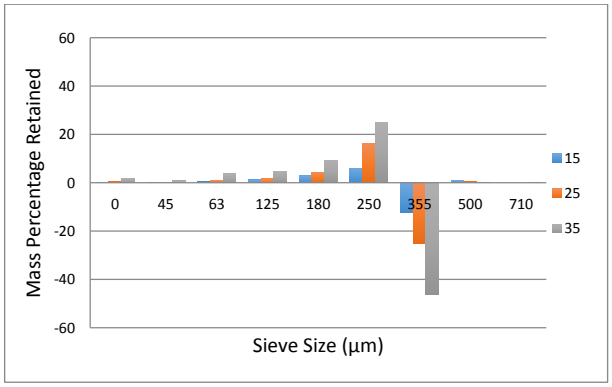

Figure 18: Mass Percentage Change of Salt under Impact Velocities (measured in m/s) for the Size Fraction 355-500 µm

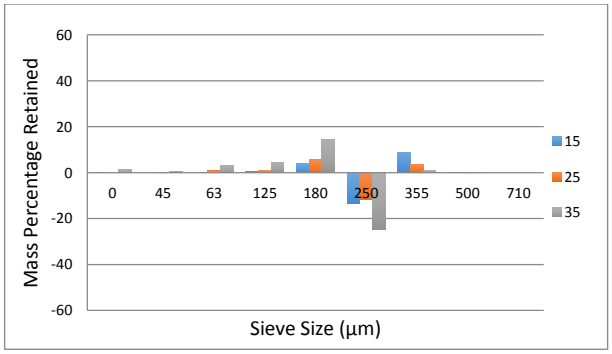

Figure 19: Mass Percentage Change of Salt under Impact Velocities (measured in m/s) for the Size Fraction 250-355 µm

Even though the size fractions considered for salt are smaller than those considered for golden breadcrumbs, the magnitude of breakage occurring is comparable under some impact velocities. For example, the amount of material lost for salt in the 355 µm size fraction tested at 35 m/s, is of the same order of magnitude as that lost for golden breadcrumbs in the 1000 µm size fraction at 35 m/s. While there is little relationship between the two materials with respect to particle size, this demonstrates the influence of the material with regard to the particle strength.

5.4. Particle Breakage Relationships

The full size distribution of a sample material post-breakage should be composed of breakage of each size fraction if a logical progression is followed. Therefore, the breakage of the narrow size fractions will be used to construct a predictive size distribution for the full distribution of material at each of the breakage velocities. The simulated size distributions will calculated from three components:

1. The percent mass of the virgin size distribution,
2. The amount of material lost in each of the size fractions tested for their breakage characteristics,
3. The amount of material contributed to each size fraction from the breakage tests address in Component 2.

This approach will make the following assumptions/limitations:

- Material collected on sieves greater than the diameter of size fractions of interest in the narrow size fraction post-breakage measurements will be omitted and treated as an error in the experimental method,
- Material in the virgin size distribution greater in diameter than that considered in narrow size fraction testing will be omitted from the results displayed, however will still be accounted for in overall sample size to calculate percentage masses of subsequent size fractions,
- Material in size fractions smaller than those tested under the narrow size fraction tests will be treated as stationary (undergo no breakage in the simulation),
- Only a limited number of size fractions will be considered in the testing regime, as addressed in Section 4.3.

The generalized equation used to calculate the simulated percentage mass retained on the sieve for a given size fraction is given in Equation 1.

$$m_{frac,sim} = m_{frac,vir} + \sum_{Frac} \left(\frac{p_{frac}}{100} \times m_{tot,sim} \right) \quad (1)$$

Where:

- $m_{frac,sim}$ is the simulated mass retained in a simulated breakage,
- $m_{frac,vir}$ is the mass retained for a given fraction in the material virgin size distribution,
- $m_{tot,sim}$ is the total sample mass of material input into the simulated breakage and is composed of the full size distribution,
- p_{frac} is the percentage change in mass of each fraction as a function of the sample mass.

Figures 20, 21 and 22 compare the experimental results (denoted by FSD) and the simulated results (denoted by SIM) for golden breadcrumbs at impact velocities of 15, 25, and 35 m/s respectively.

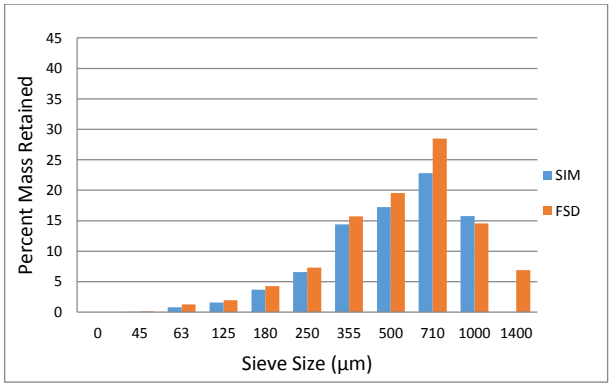

Figure 20: Simulated and Experimental Post-Test Golden Breadcrumb Size Distributions at 15 m/s Impact Velocity

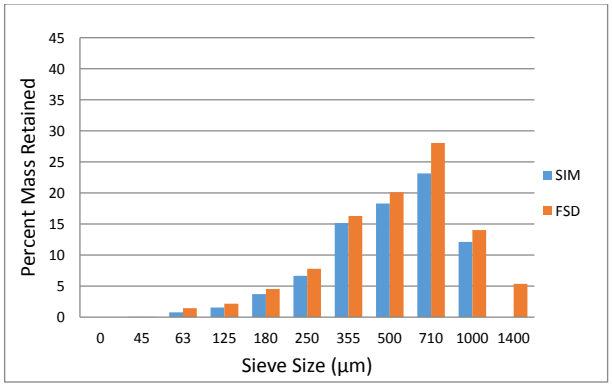

Figure 21: Simulated and Experimental Post-Test Golden Breadcrumb Size Distributions at 25 m/s Impact Velocity

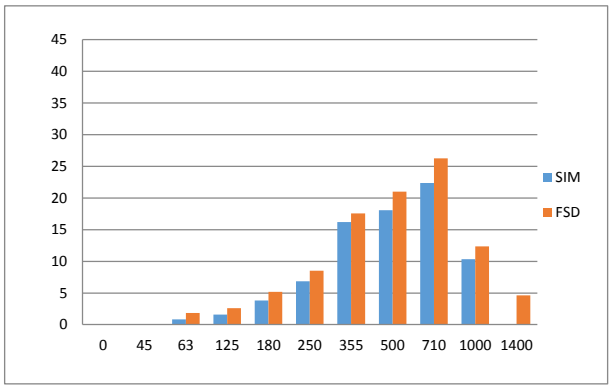

Figure 22: Simulated and Experimental Post-Test Golden Breadcrumb Size Distributions at 35 m/s Impact Velocity

Considering the assumptions made in the simulation method, the predictions made fit reasonably well with the full size distribution breakage results. The most notable differences that can be observed lie primarily in the larger size fractions, namely 710 and 1000 µm. This observation is expected, as the 1400 µm size fraction was not considered in the narrow size fraction breakage analysis. It would be logically sound to state that this size fraction would contribute to the 710 and 1000 µm fractions, increasing agreement between the simulated and experimental values.

With regard to the smaller size fractions, the simulation underestimates the magnitude consistently. This may be explained by the simulation failing to account for the movement of all size fractions below those for which results are presented. It is expected that all fractions will break to some degree, thus contributing to the stated error.

By taking into consideration both of the aforementioned statements, the accuracy of the simulated predictions could be increased.

Figures 23, 24 and 25 compare the experimental results (denoted by FSD) and the simulated results (denoted by SIM) for salt, at impact velocities of 15, 25, and 35 m/s respectively.

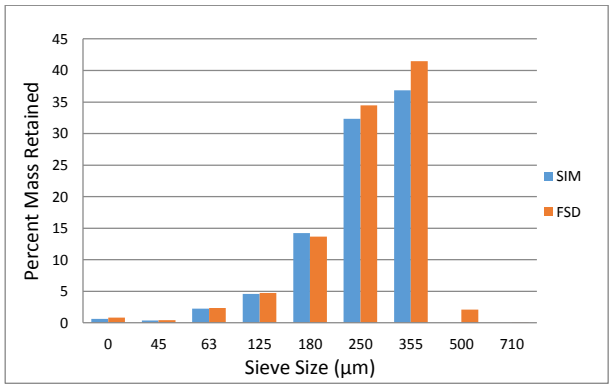

Figure 23: Simulated and Experimental Post-Test Salt Size Distributions at 15 m/s Impact Velocity

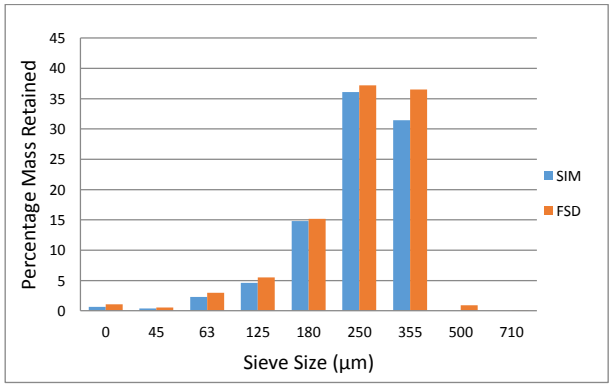

Figure 24: Simulated and Experimental Post-Test Salt Size Distributions at 25 m/s Impact Velocity

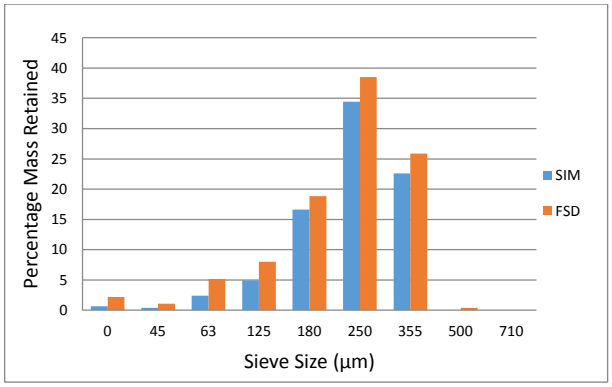

Figure 25: Simulated and Experimental Post-Test Salt Size Distributions at 35 m/s Impact Velocity

As with the golden breadcrumbs, a good agreement between the simulated and experimental results for salt is achieved. Almost all size fractions are under-predicted once again, and as with the golden breadcrumbs, the logical explanations for this behavior lie with the omission of larger size fractions than what underwent testing, in addition to the migration of smaller size fractions.

6. CONCLUSIONS

Research into the breakage characteristics of two granulated food products, one crystalline in structure and the other non-crystalline, has been performed. The virgin size distributions were determined, and then the resulting size distributions were tested under three impact velocities: 15, 25 and 35 m/s. Subsequently, three size fractions for golden breadcrumbs and two size fractions for salt were tested under the same conditions as the full size distributions. The results of the latter tests were used to simulate the conditions of the full size distribution breakage characteristics.

The simulated results found good agreement across each of the two materials and the three impact velocities considered. The discrepancies between the experimental and simulated results have been attributed to a combination of omitting the larger size fractions not considered in the testing, and neglecting the migration of the smaller size fractions down the material size distribution. Both discrepancies may be addressed with further testing.

7. FUTURE DIRECTION

The future direction of this work falls primarily into two categories: enhancing the predictive capabilities of this method of analysis, and to enhance understanding of how this analysis may be used in the design and/or optimization process.

Enhancing the predictive capabilities of this method includes looking more holistically at the size distribution and testing the breakage characteristics of every available size fraction. From this, increasing the accuracy of the final size distribution prediction should be achievable.

The application of this analysis would involve obtaining a greater understanding of the process in question, subsequently followed by identifying the undesirable material qualities that result from excess attrition. Determining the ratio of size fractions that exhibit these undesirable qualities will then enable quantification of the process conditions to be avoided.

ACKNOWLEDGEMENTS

The author would like to express gratitude for the valuable input of others in this programme of research. In particular, Mr Jonathon Larkin for his technical advice, and Mrs Caroline Chapman for her administrative assistance. Without their support, this work would not be possible.

REFERENCES

Bridle I., 2000. The analysis of particle degradation in pneumatic conveyors utilizing a pilot-sized test facility. Thesis (PhD). University of Greenwich.

Burnett A.J., 1996. The use of laboratory erosion tests for the prediction of wear in pneumatic conveying bends. Thesis (PhD). University of Greenwich.

Chapelle P., Abou-Chakra H., Christakis N., Patel M., Abu-Nahar A., Tüzün U., Cross M., 2004. Computational model for prediction of particle degradation during dilute-phase pneumatic conveying: the use of a laboratory-scale degradation tester for the determination of degradation propensity. Advanced Powder Technology, 15 (1), 13-29.

Deng T., Li J., Chaudhry A.R., Patel M., Hutchings I., Bradley M.S.A., 2005. Comparison between weight loss of bends in a pneumatic conveyor and erosion rate obtained in a centrifugal erosion tester for the same materials. Wear, 258, 402-411.

Kalman H., 2000. Attrition of powders and granules at various bends during pneumatic conveying. Powder Technology, 112, 244-250.

Macchini R., Bradley M.S.A., Deng T., 2013. Influence of particle size, density, particle concentration on bend erosive wear in pneumatic conveyors. Wear, 303, 21-29.

Sato S., Shimizu A., Yokomine T., 1995. Numerical prediction of erosion for suspension flow duct. Wear, 186-187, 203-209.

van Laarhoven B., Schaafsma S.H., Meesters G.M.H., 2012. Towards a desktop attrition tester; validation with dilute phase pneumatic conveying. Chemical Engineering Science, 73, 321-328.

AUTHOR'S BIOGRAPHY

Benjamin Kotzur commenced his PhD research at The Wolfson Centre for Bulk Solids Handling Technology, at the University of Greenwich, in May 2014. Having grown up in a family business designing bulk solids storage and handling facilities, he completed his Bachelor of Engineering (Scholars) (Honors) at the University of Wollongong, Australia, with a focus on modelling of bulk materials in dynamic systems. He specialises in the measurement and prediction of particle attrition during lean phase pneumatic conveying, however, he retains a keen interest in all bulk solids handling processes, across a vast range of industrial and academic spheres.